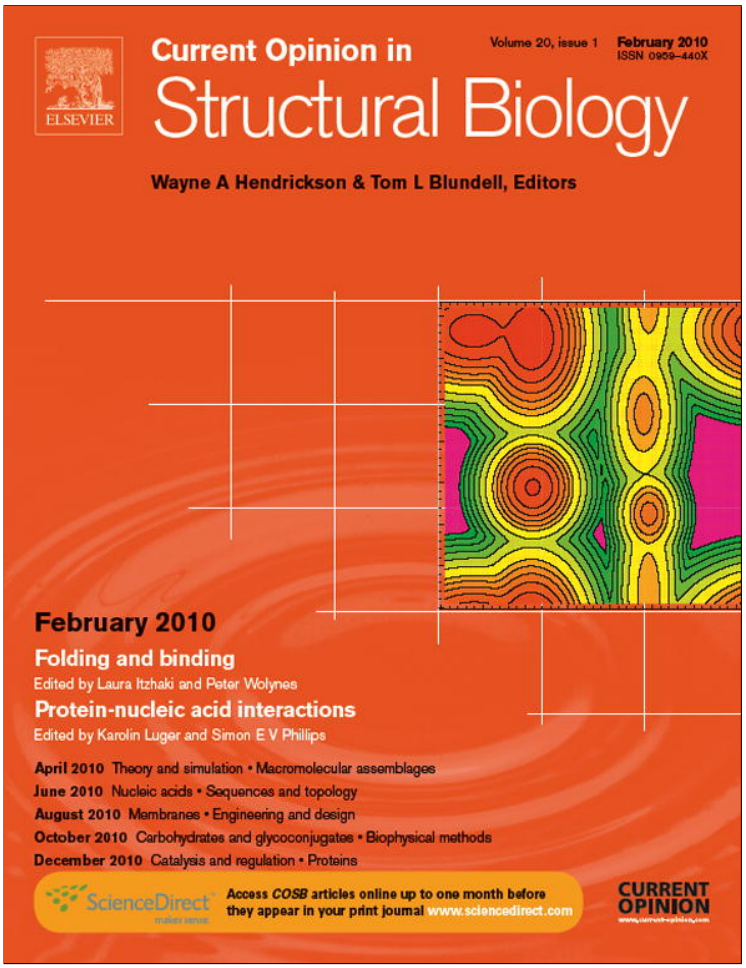

Available online at www.sciencedirect.com
ScienceDirect
Current Opinion in Structural Biology

Energy landscapes: some new horizons

David J Wales

Kinetic transition networks can now be calculated for small proteins using geometry optimisation to characterise minima, transition states and pathways, and unimolecular rate theory to supply rate constants corresponding to each transition state. The networks can be visualised by constructing disconnectivity graphs, revealing striking differences between good structure-seeking systems and a model glass former. The glassy landscape contains competing low-lying minima separated by high barriers, providing a more extreme example of the frustration previously characterised for model proteins. Free energy projections that preserve barriers and rates can be obtained from the network representation, and global kinetics can be addressed on the experimental time scale.

Address
University Chemical Laboratories, Lensfield Road, Cambridge CB2 1EW, UK

Corresponding author: Wales, David J (dw34@cam.ac.uk)

Current Opinion in Structural Biology 2010, **20**:3–10

This review comes from a themed issue on
Folding and binding
Edited by Laura Itzhaki and Peter Wolynes

Available online 22nd January 2010

0959-440X/$ – see front matter

DOI 10.1016/j.sbi.2009.12.011

Introduction

Representing a potential energy surface (PES) in terms of local minima and the transition states that connect them provides a convenient coarse-grained representation of the corresponding landscape [1]. Such networks can be constructed using geometry optimisation techniques, providing a complementary approach to molecular dynamics and Monte Carlo simulations. Locating pathways corresponding to high barriers is generally no harder than characterising low-barrier processes, providing insight into rearrangements that occur on long time scales. The overall organisation of the landscape can then be visualised using disconnectivity graphs [2], and when rate constants are associated with the rearrangements mediated by each transition state we can define a kinetic transition network [3••,4•].

The disconnectivity graph approach was first applied to a database of local minima and transition states for a tetrapeptide, which had previously been employed in a master equation analysis of the global dynamics [5]. Disconnectivity graphs constructed from existing databases for atomic and molecular clusters immediately identified several motifs associated with distinct classes of generic kinetic and thermodynamic properties [6]. Over the last decade improvements in geometry optimisation algorithms and database analysis have made it possible to treat networks containing more than a million local minima [1,7]. Programmes to construct, analyse and visualise the potential energy landscape can be downloaded from URL http://www-wales.ch.cam.ac.uk/software.html for use under the GNU General Public License.

Contrasting landscapes

Some recent results are collected in Figure 1 to illustrate the common features revealed for good 'structure-seeking' systems, and to contrast these with a glassy potential energy landscape. The graphs in Figure 1(a)–(d) correspond to $T = 1$ and 3 icosahedral shells composed of rigid pentagonal and hexagonal pyramids [8,9], the 16-residue GB1 peptide [10], which forms a β-hairpin in the full B1 domain of protein G [11] and in solution [12–14], and the 20-residue miniprotein beta3s [15•], which was designed to adopt a three-stranded antiparallel β-sheet conformation [16]. The vertical axis in each graph represents potential or free energy, and the spacing of branches on the horizontal axis is chosen to reveal the structure as clearly as possible. The branches terminate at the energies defined by individual potential energy minima, or groups of minima in the case of the GB1 peptide, and are joined together at energy thresholds where the barriers separating different sets can be overcome [2].

The graphs in panels (a)–(d) have a 'palm tree' structure, with a well-defined global potential energy minimum, and low downhill barriers from higher lying minima. This motif is also associated with efficient relaxation to 'magic number' clusters in molecular beams [1,6,17], and with crystallisation [17]. Such potential energy landscapes have 'funnelling' properties, since there is generally a well-defined free energy minimum that is kinetically accessible over a wide range of temperature. To establish this connection directly requires additional calculations, since the entropy is determined by the potential energy distribution of local minima and their vibrational densities of states [17], as discussed below. The graphs in Figure 1(a)–(d) could also be described in terms of a 'folding funnel' [18–20] defined in terms of a set of convergent kinetic pathways [21]. In contrast, the graph for a model glass former [Figure 1(e)] is qualitatively

Figure 1

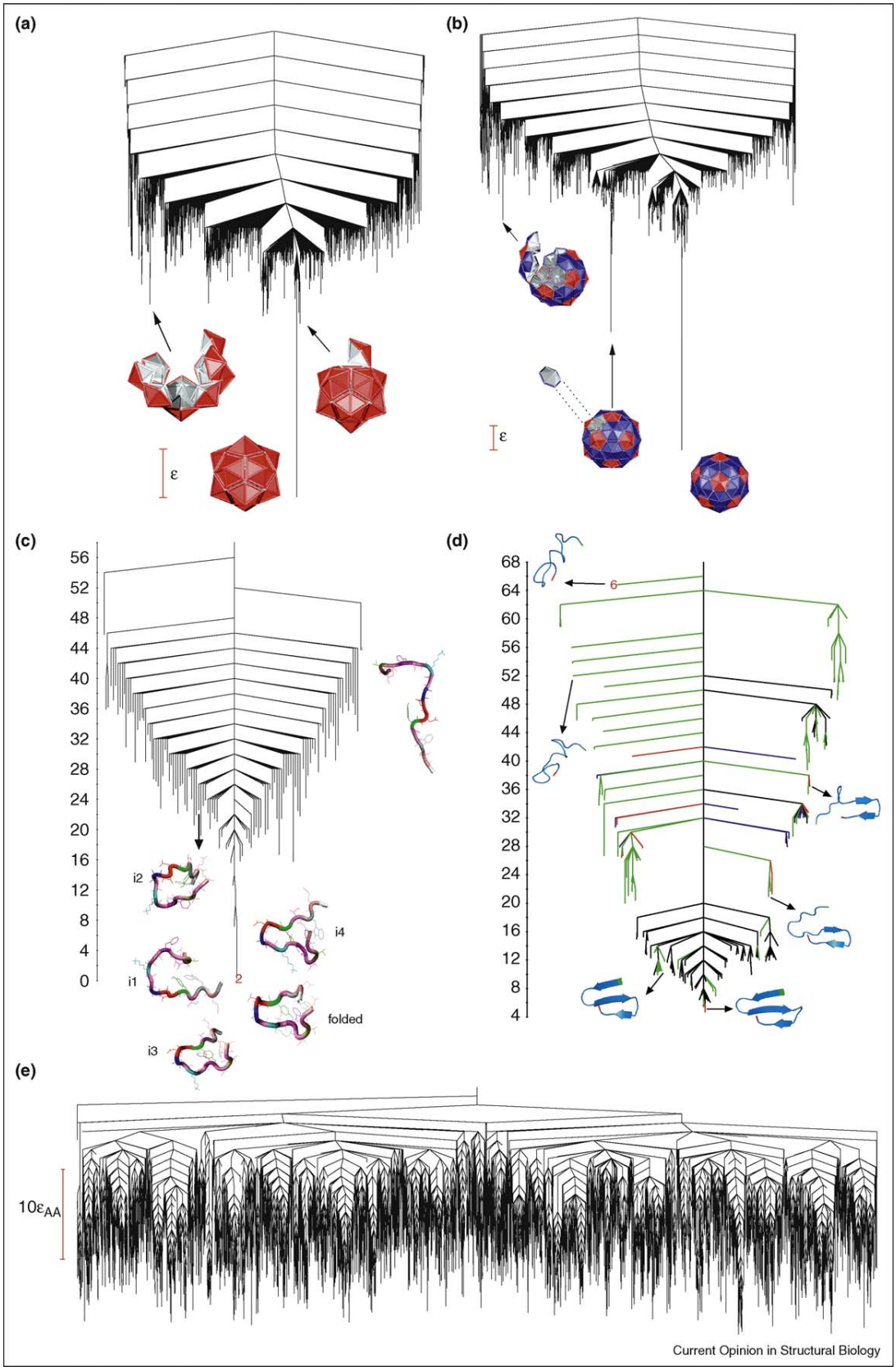

Figure 2

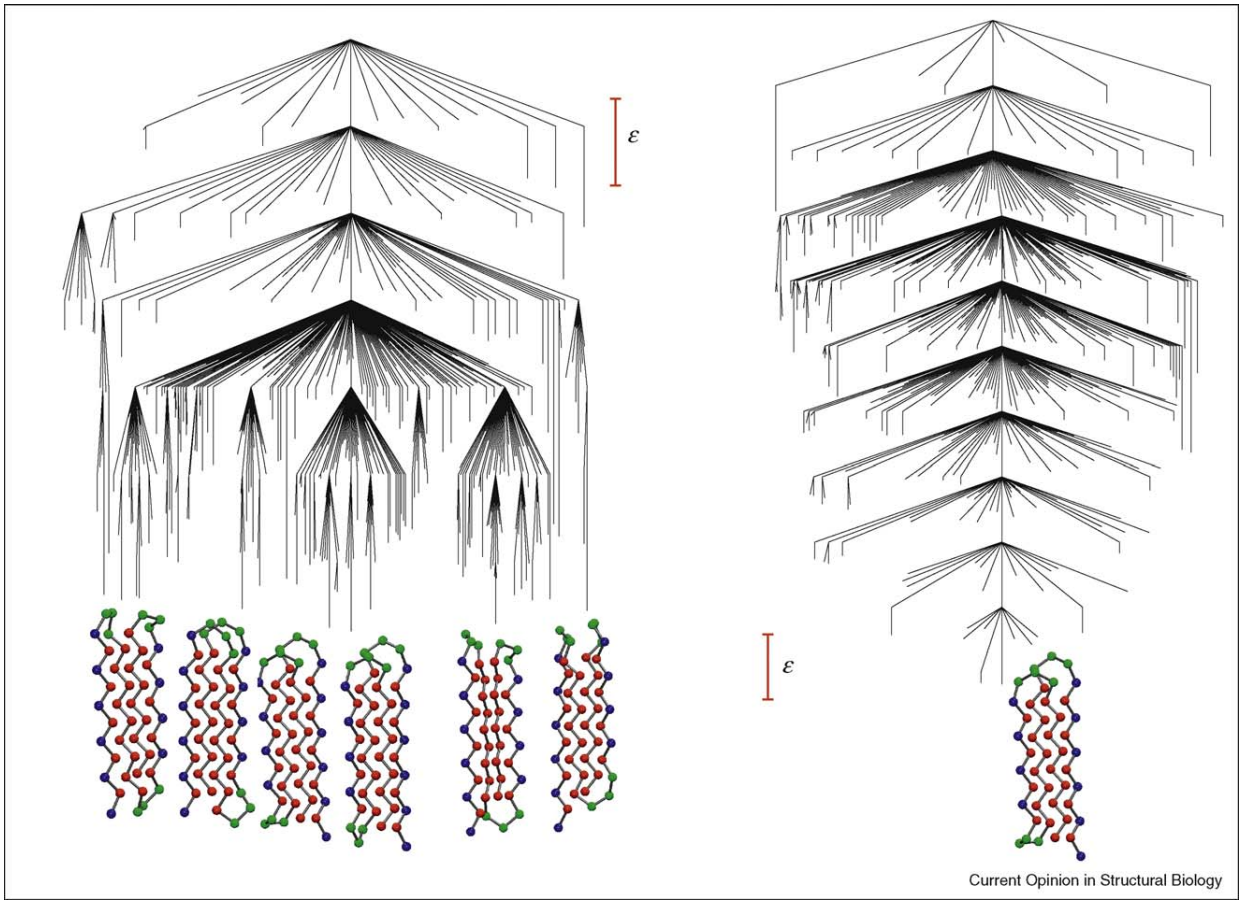

The global minimum of the off-lattice bead model with sequence $B_9N_3(LB)_4N_3B_9N_3(LB)_5L$ is a four-stranded β-barrel, where B=hydrophobic; L=hydrophilic; and N=neutral [25]. The original system exhibits frustration, as shown by the alternative β-barrel minima separated by high barriers in the disconnectivity graph on the left. The frustration is eliminated in the graph for the corresponding Gō model [24] on the right, and is also reduced by salt bridges [28,29]. ϵ is the unit of energy, which has been assigned a value of around 1 kJ/mol in previous work.

different [22]. Here the lowest lying amorphous minima are separated by potential energy barriers that are very large compared to k_BT at the glass transition, leading to ergodicity breaking on accessible experimental and simulation time scales. The alternative low-lying minima separated by high barriers correspond to a rugged, frustrated landscape, in contrast to the minimal frustration [18,23] expected for a good structure-seeking system.

Visualising frustration

The effect of removing favourable interactions that are not present in the global minimum to make a Gō model is illustrated for a model 46-residue protein in Figure 2 [24]. The original off-lattice bead potential was designed to exhibit frustration in the form of competing β-barrel structures separated by high barriers [25–27]. In the Gō model these alternative structures are no longer competi-

(Figure 1 Legend) Disconnectivity graphs for good structure-seeking systems [panels **(a)**–**(d)**] contrast strongly with a glassy system [panel **(e)**]. The graphs in (a) and (b) correspond to global minima with icosahedral symmetry and triangulation numbers (a) $T = 1$ and (b) $T = 3$ [9]. ϵ is the pair well depth for the interaction between two equatorial sites of different pyramids. (c) Free energy (kcal/mol) disconnectivity graph calculated at 298 K for the GB1 peptide using an implicit solvent and a barrier threshold of 5 kcal/mol for regrouping [10]. Structures corresponding to one member of the denatured set and five members of the expanded group of folded states are superimposed on the graph. (d) Potential energy (kcal/mol) disconnectivity graph for beta3s based on the stationary points that appear in the 250 fastest discrete paths [15•]. The branches are coloured according to whether the corresponding local minima appear in the fastest or slowest of these paths, revealing that only minor differences in the folding pathway occur within this set. Green branches lead to minima present in both the fastest and slowest paths in the set, red branches correspond to minima on the fastest path, but not the slowest, and blue branches correspond to minima on the slowest path, but not the fastest [15•]. (e) Disconnectivity graph calculated for the minima sampled [22] over a locally ergodic time interval in a binary Lennard-Jones system of 60 particles (12 of type B and 48 of type A) modelled with periodic boundary conditions at a number density of 1.3 and $k_BT/\epsilon_{AA} = 0.96$. Here, ϵ_{AA} is the pair well depth between atoms of type A.

tive, and the disconnectivity graph now corresponds to an efficient structure-seeker [24]. Introducing salt bridges at key sites produces landscapes with intermediate character, which is reflected in both explicit dynamical simulations [28] and in the mean first-encounter time for global optimisation [29]. This 46-bead model has provided a number of useful insights into the interplay of frustration, dynamics and thermodynamics [28,30–31,32•].

Visualising the potential energy landscape for systems that locate a particular structure efficiently has helped to unify our understanding of how non-random searches guide self-assembly, folding, crystallisation and the appearance of magic numbers for clusters in a molecular beam [1,6,17]. The disconnectivity graph can be viewed as a convenient summary of the underlying kinetic transition network [3••,4•], and quantitative results for global thermodynamic and kinetic properties can be obtained from the connectivity information and densities of states corresponding to the underlying stationary points [1,17]. The graphs can also be analysed in terms of basic network properties, such as the distribution of the number of connections for each local minimum. Landscapes corresponding to efficient structure-seekers may exhibit scale-free properties, where a highly connected global minimum acts as a hub to give a power law probability distribution for the number of connections [33,34].

Extracting global thermodynamic and kinetic properties

The disconnectivity graph approach can be extended to represent free energy rather than potential energy [35,36], and graphs can also be constructed using transition probabilities obtained from explicit dynamics [37••]. These representations avoid the problems that can sometimes arise for free energy surfaces corresponding to low-dimensional projections, which can misrepresent or even remove barriers [3••,38–41]. Integrating over all but one or two degrees of freedom can produce distributions where the connectivity information that determines transition rates is lost. In particular, if we choose an inappropriate order parameter that averages over states on different sides of a high barrier, then kinetically isolated configurations can appear to be connected. Similar problems may arise in rare event calculations [42,43].

A kinetic transition network defined in terms of stationary points of the PES retains all the connectivity information, which can be faithfully represented using a free energy disconnectivity graph [35,36]. It is also possible to define a progress coordinate from the underlying network that preserves the barriers [35,39]. Using harmonic or anharmonic densities of states for each local minimum, j, of the PES enables us to calculate the corresponding partition function, $Z_j(T)$, or free energy at any given temperature, T. Each minimum of the PES then corresponds to a local free energy minimum, but projection onto a lower dimensional space can produce surfaces with a much simpler appearance [17]. Alternatively, the local free energy minima, and the transition states that connect them, can be grouped together if they are separated by barriers below a given threshold [1,15,36,44,45]. We then define the free energy of group J as

$$F_J(T) = -k_B T \ln \sum_{j \in J} Z_j(T), \tag{1}$$

and the free energy of the group of transition states (†) that links group J to group L as

$$F^{\dagger}_{LJ}(T) = -k_B T \ln \sum_{l \leftarrow j} Z^{\dagger}_{lj}(T) \equiv -k_B T \ln Z^{\dagger}_{LJ}(T). \tag{2}$$

The inter-group rate constant from J to L, k_{LJ}, is then [45]:

$$k_{LJ}(T) = \sum_{l \leftarrow j} \frac{p_j^{\mathrm{eq}}(T)}{p_J^{\mathrm{eq}}(T)} k_{lj}(T) = \sum_{l \leftarrow j} \frac{Z_j(T)}{Z_J(T)} \frac{k_B T}{h} \frac{Z^{\dagger}_{lj}(T)}{Z_j(T)}$$
$$= \frac{k_B T}{h} \frac{Z^{\dagger}_{LJ}(T)}{Z_J(T)} = \frac{k_B T}{h} e^{-\left[F^{\dagger}_{LJ}(T) - F_J(T)\right]/k_B T}.$$

The effect of this regrouping scheme is illustrated for the alanine dipeptide in Figure 3.

A formally exact expression for the global equilibrium partition function can be obtained using the superposition formula [1,46••], which is a sum over non-overlapping contributions from all the local minima on the PES:

$$Z(T) = \sum_j Z_j(T). \tag{3}$$

This result is usually combined with approximate expressions for the local densities of states [1], and for problems involving broken ergodicity it can provide accurate thermodynamic properties many orders of magnitude faster than techniques such as parallel tempering [47]. The superposition approach can also be used to project the free energy onto a chosen order parameter, a, using partition functions that involve a Gaussian shape function [46••]:

$$Z_j(a, T) = \left(\frac{k_B T}{h \bar{\nu}_j}\right)^{\kappa} \frac{\exp\left(-V_j/k_B T\right)}{\sqrt{2\pi k_B T A_j}} \exp\left[-\frac{(a - a_j)^2}{2 k_B T A_j}\right], \tag{4}$$

where $\bar{\nu}_j$ is the geometric mean of the normal mode vibrational frequencies, $\nu_{j,\gamma}$, of minimum j, with potential energy V_j and order parameter a_j. $\kappa = 3N - 6$, where N is the number of atoms, and

$$A_j = \sum_{\gamma=1}^{\kappa} \left[\left.\frac{\partial a(\mathbf{q}_j)}{\partial q_{j,\gamma}}\right|_{\mathbf{q}_j = \mathbf{0}} \frac{1}{2\pi \nu_{j,\gamma}}\right]^2 \tag{5}$$

Figure 3

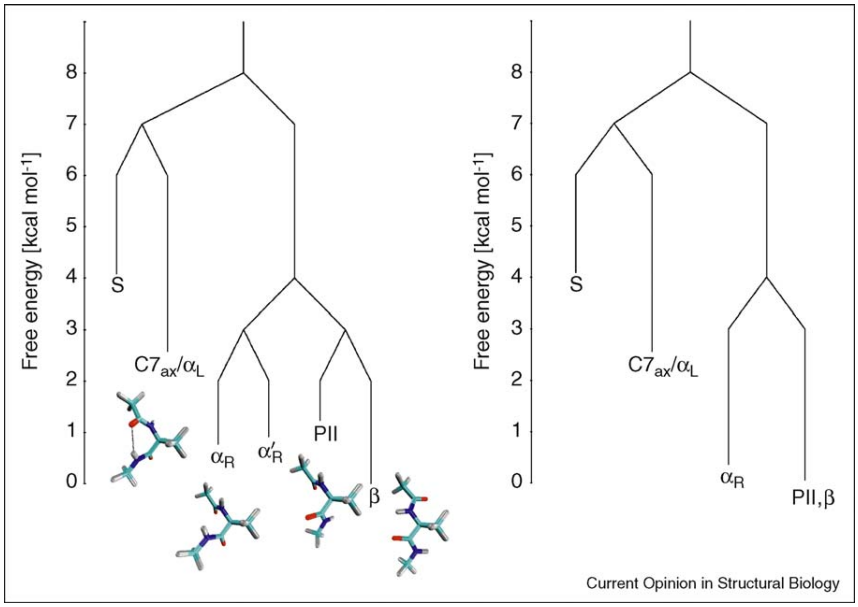

Illustration of regrouping for an implicit solvent model of alanine dipeptide. The graph on the left contains branches corresponding to all the local minima, while some structures merge together in the graph on the right [46••], which corresponds to a regrouping barrier threshold of 3 kcal/mol. The structures of the $C7_{ax}$, α_R, PII and β configurations are illustrated below the corresponding branches. In fact, the $C7_{ax}/\alpha_L$ minimum has an intermediate structure for the potential in question: the $C7_{ax}$ structure is shown for reference.

for normal modes $q_{j,\gamma}$. Projections onto multiple order parameters can also be derived [46••]. The resulting free energy surface for alanine dipeptide at room temperature in vacuum is compared with a replica exchange calculation in Figure 4 [46••]. This example illustrates a case where there is a one-to-one correspondence between the potential energy and free energy minima. However, the surfaces obtained from replica exchange and from the superposition sum are undefined in some of the barrier regions. The third panel in Figure 4 was obtained using a new reaction path Hamiltonian superposition approach (RPHSA), which includes contributions from configur-

Figure 4

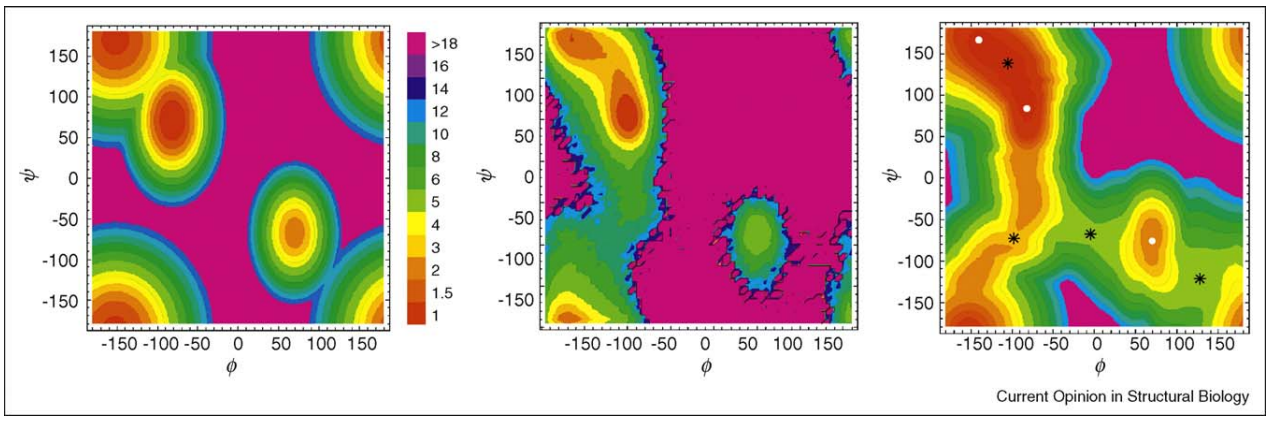

Free energy surfaces calculated for alanine dipeptide in vacuum as a function of the ϕ and ψ backbone dihedral angles using (left to right) the superposition, replica exchange, and reaction path Hamiltonian superposition techniques [46••]. The colour key free energy values are in kcal/mol. The three minima, marked by white dots in the right panel, are $C7_{eq}$, the β state and $C7_{ax}$, and the four black stars mark the transition states. Additional configurations along the paths between the minima and transition states were used in the reaction path Hamiltonian superposition calculation [46••].

ations that correspond to displacements, δ_r, from transition states, †, along pathways between local minima [46••]:

$$Z_r^\dagger(a,T) = \left(\frac{k_B T}{h}\right)^\kappa \frac{\delta_r \exp\left(-V_r^\dagger/k_B T\right)}{\left(\bar{\nu}_r^\dagger\right)^{\kappa-1} 2\pi k_B T \sqrt{A_r^\dagger}} \exp\left[-\frac{\left(a-a_r^\dagger\right)^2}{2k_B T A_r^\dagger}\right]. \quad (6)$$

Complete RPHSA calculations for dialanine in implicit solvent or vacuum require less than a minute of computer time [46••]. This performance is probably similar to the single-sweep method [48•], which involves an expansion based on explicit sampling around chosen configurations. Using geometry optimisation-based approaches to guide efficient sampling schemes could form the basis for new hybrid methodology in future work. The superposition and RPHSA results shown in the figure include only the enantiomers corresponding to the L-conformations of each amino acid. The D-forms are located as well, but are omitted from the calculations to facilitate comparison with replica exchange, where these isomers are not encountered because of incomplete sampling.

Mean first-passage times and rate constants can also be extracted from kinetic transition networks [3••,4•,7,49], complementing simulation methods for rare events based on explicit dynamics [37••,43,50–54]. Rate constants and representative pathways have been calculated from the databases corresponding to the disconnectivity graphs in Figure 1 for the GB1 peptide [10] and beta3s miniprotein [15•]. For both systems the sequence of events involved in folding and the calculated rate constants agree with previous work [13,14,16,37••,44,55–58,59•,60]. Single molecule experiments [61•] provide new targets for future computational studies, which together will produce more detailed insight into how biomolecules attain their native states [62,63].

Outlook

Advances in geometry optimisation techniques, global optimisation algorithms, and Monte Carlo and molecular dynamics sampling have provided complementary insight into the energy landscapes of biomolecules [1]. Further improvements in the underlying force fields and simulation methodology can be anticipated in the future. However, an important conceptual issue remains to be resolved, namely how details of the interatomic and intermolecular potential determine the characteristics of the underlying PES. Here the tools of catastrophe theory can be employed, which provide a general framework for understanding how parameter changes affect the organisation of the landscape. Initial work for atomic clusters has identified how short-range potentials produce landscapes that are locally rougher, in terms of the number of local minima, but globally flatter [64]. Short-range potentials can therefore hamper both the kinetic and thermodynamic factors that are required for efficient relaxation. The extension of this framework to anisotropic molecular and biomolecular force fields is now in progress.

Acknowledgements

I am grateful to Prof D Frenkel, Dr B Strodel and Dr M Miller for their comments on the original version of this article, as well as the authors of the highlighted references. Some of this research was supported by the BBSRC, the EPSRC and the Gates Trust.

References and recommended reading

Papers of special interest, published within the period of review, have been highlighted as:

- • of special interest
- •• of outstanding interest

1. Wales DJ: *Energy Landscapes*. Cambridge: Cambridge University Press; 2003.

2. Becker OM, Karplus M: **The topology of multidimensional potential energy surfaces: theory and application to peptide structure and kinetics**. *J Chem Phys* 1997, **106**:1495-1515.

3. •• Noé F, Fischer S: **Transition networks for modeling the kinetics of conformational change in macromolecules**. *Curr Opin Struct Biol* 2008, **18**:154-162.
A summary and comparison of how kinetic transition networks are constructed from geometry optimisation and molecular dynamics simulations.

4. • Prada-Gracia D, Gómez-Gardenes J, Echenique P, Fernando F: **Exploring the free energy landscape: from dynamics to networks and back**. *PLoS Comput Biol* 2009, **5**:1-9.
The authors employ a molecular dynamics approach to construct a 'Conformational Markov network' and apply their approach to the alanine dipeptide.

5. Czerminski R, Elber R: **Reaction path study of conformational transitions in flexible systems: applications to peptides**. *J Chem Phys* 1990, **92**:5580-5601.

6. Wales DJ, Miller MA, Walsh TR: **Archetypal energy landscapes**. *Nature* 1998, **394**:758-760.

7. Wales DJ: **Energy landscapes: calculating pathways and rates**. *Int Rev Phys Chem* 2006, **25**:237-282.

8. Wales DJ: **The energy landscape as a unifying theme in molecular science**. *Phil Trans Roy Soc A* 2005, **363**:357-377.

9. Fejer S, James T, Hernandez-Rojas J, Wales DJ: **Energy landscapes for shells assembled from pentagonal and hexagonal pyramids**. *Phys Chem Chem Phys* 2009, **11**:2098-2104.

10. Carr JM, Wales DJ: **Refined kinetic transition networks for the GB1 hairpin peptide**. *Phys Chem Chem Phys* 2009, **11**:3341-3354.

11. Gronenborn AM, Filpula DR, Essig NZ, Achari A, Whitlow M, Wingfield PT, Clore GM: **A novel, highly stable fold of the immunoglobulin binding domain of streptococcal protein G**. *Science* 1991, **253**:657-661.

12. Blanco FJ, Rivas G, Serrano L: **A short linear peptide that folds into a native stable beta-hairpin in aqueous solution**. *Nat Struct Biol* 1994, **1**:584-590.

13. Muñoz V, Thompson PA, Hofrichter J, Eaton WA: **Folding dynamics and mechanism of β-hairpin formation**. *Nature* 1997, **390**:196-199.

14. Olsen KA, Fesinmeyer RM, Stewart JM, Andersen NH: **Hairpin folding rates reflect mutations within and remote from the turn region**. *Proc Natl Acad Sci U S A* 2005, **102**:15483-15487.

15. • Carr JM, Wales DJ: **Folding pathways and rates for the three-stranded beta-sheet peptide beta3s using discrete path sampling**. *J Phys Chem B* 2008, **112**:8760-8769.
The discrete path sampling approach is used to construct a kinetic transition network from local minima and transition states of the potential energy surface for the beta3s miniprotein, The sequence of folding events

is analysed for the paths that make the largest contribution to the folding rate constant.

16. de Alba E, Santoro J, Rico M, Jiménez MA: **Measuring the refolding of β-sheets with different turn sequences on a nanosecond time scale**. *Protein Sci* 1999, **8**:854-865.

17. Wales DJ, Bogdan TV: **Potential energy and free energy landscapes**. *J Phys Chem B* 2006, **110**:20765-20776.

18. Bryngelson JD, Onuchic JN, Socci ND, Wolynes PG: **Funnels, pathways, and the energy landscape of protein folding: a synthesis**. *Proteins* 1995, **21**:167-195.

19. Onuchic JN, Wolynes PG, Luthey-Schulten Z, Socci ND: **Toward an outline of the topography of a realistic protein-folding funnel**. *Proc Natl Acad Sci U S A* 1995, **92**:3626-3630.

20. Onuchic JN, Nymeyer H, García AE, Chahine J, Socci ND: **The energy landscape theory of protein folding: insights into folding mechanisms and scenarios**. *Adv Protein Chem* 2000, **53**:87-152.

21. Leopold PE, Montal M, Onuchic JN: **Protein folding funnels: a kinetic approach to the sequence–structure relationship**. *Proc Natl Acad Sci U S A* 1992, **89**:8721-8725.

22. de Souza VK, Wales DJ: **Diagnosing broken ergodicity using an energy fluctuation metric**. *J Chem Phys* 2005, **123**:134504.

23. Onuchic JN, Luthey-Schulten Z, Wolynes PG: **Theory of protein folding: the energy landscape perspective**. *Annu Rev Phys Chem* 1997, **48**:545-600.

24. Miller MA, Wales DJ: **Energy landscape of a model protein**. *J Chem Phys* 1999, **111**:6610-6616.

25. Honeycutt JD, Thirumalai D: **Metastability of the folded states of globular proteins**. *Proc Natl Acad Sci U S A* 1990, **87**:3526-3529.

26. Guo Z, Brooks CL III: **Thermodynamics of protein folding: a statistical mechanical study of a small all-β protein**. *Biopolymers* 1997, **42**:745-757.

27. Berry RS, Elmaci N, Rose JP, Vekhter B: **Linking topography of its potential surface with the dynamics of folding of a protein model**. *Proc Natl Acad Sci U S A* 1997, **94**:9520-9524.

28. Stoycheva AD, Onuchic JN, Brooks CL: **Effect of gatekeepers on the early folding kinetics of a model beta-barrel protein**. *J Chem Phys* 2003, **119**:5722-5729.

29. Wales DJ, Dewsbury PEJ: **Effect of salt bridges on the energy landscape of a model protein**. *J Chem Phys* 2004, **121**:10284-10290.

30. Nymeyer H, García AE, Onuchic JN: **Folding funnels and frustration in off-lattice minimalist protein landscapes**. *Proc Natl Acad Sci U S A* 1998, **95**:5921-5928.

31. Shea JE, Onuchic JN, Brooks CL: **Energetic frustration and the nature of the transition state**. *J Chem Phys* 2000, **113**:7663-7671.

32. • Kim J, Keyes T, Straub JE: **Relationship between protein folding thermodynamics and the energy landscape**. *Phys Rev E* 2009, **79**:030902R.

A detailed connection is developed between the potential energy landscape of a coarse-grained protein model and the observed thermodynamic properties.

33. Doye JPK: **Network topology of a potential energy landscape: a static scale-free network**. *Phys Rev Lett* 2002, **88**:238701.

34. Rao F, Caflisch A: **The protein folding network**. *J Mol Biol* 2004, **342**:299-306.

35. Krivov SV, Karplus M: **Free energy disconnectivity graphs: application to peptide models**. *J Chem Phys* 2002, **117**:10894-10903.

36. Evans DA, Wales DJ: **Free energy landscapes of model peptides and proteins**. *J Chem Phys* 2003, **118**:3891-3897.

37. •• Krivov SV, Muff S, Caflisch A, Karplus M: **One-dimensional barrier-preserving free-energy projections of a beta-sheet miniprotein: new insights into the folding process**. *J Phys Chem B* 2008, **112**:8701-8714.

Molecular dynamics simulations are used to construct a free energy profile for the beta3s miniprotein. p_{fold} analysis is compared with a free energy projection that is specifically designed to preserve barriers.

38. Krivov SV, Karplus M: **Hidden complexity of free energy surfaces for peptide (protein) folding**. *Proc Nat Acad Sci U S A* 2004, **101**:14766-14770.

39. Krivov SV, Karplus M: **One-dimensional free-energy profiles of complex systems: progress variables that preserve the barriers**. *J Phys Chem B* 2006, **110**:12689-12698.

40. Muff S, Caflisch A: **Kinetic analysis of molecular dynamics simulations reveals changes in the denatured state and switch of folding pathways upon single-point mutation of a β-sheet miniprotein**. *Proteins Struct Funct Bioinf* 2008, **70**:1185-1195.

41. Krivov SV, Karplus M: **Diffusive reaction dynamics on invariant free energy profiles**. *Proc Natl Acad Sci U S A* 2008, **105**:13841-13846.

42. Dickson BM, Makarov DE, Henkelman G: **Pitfalls of choosing an order parameter for rare event calculations**. *J Chem Phys* 2009, **131**:074108.

43. Bolhuis PG, Chandler D, Dellago C, Geissler PL: **Transition path sampling: throwing ropes over rough mountain passes, in the dark**. *Annu Rev Phys Chem* 2002, **53**:291-318.

44. Evans DA, Wales DJ: **Folding of the GB1 hairpin peptide from discrete path sampling**. *J Chem Phys* 2004, **121**:1080-1090.

45. Carr JM, Wales DJ: **Global optimization and folding pathways of selected alpha-helical proteins**. *J Chem Phys* 2005, **123**:234901.

46. •• Strodel B, Wales DJ: **Free energy surfaces from an extended harmonic superposition approach and kinetics for alanine dipeptide**. *Chem Phys Lett* 2008, **466**:105-115.

Free energy surfaces are calculated and compared for the alanine dipeptide using a number of different potentials and implicit solvent representations. The analysis starts with global optimisation and includes rate constant calculations for each rearrangement. The reaction path Hamiltonian superposition approach is introduced and employed to project the free energy onto two internal coordinates.

47. Sharapov VA, Meluzzi D, Mandelshtam VA: **Low-temperature structural transitions: circumventing the broken-ergodicity problem**. *Phys Rev Lett* 2007, **98**:105701.

48. • Maragliano L, Vanden-Eijnden E: **Single-sweep methods for free energy calculations**. *J Chem Phys* 2008, **128**:184110.

A temperature-accelerated molecular dynamics simulation is employed to survey the potential energy surface, followed by a local expansion and sampling of the free energy surface.

49. Noé F, Krachtus D, Smith JC, Fischer S: **Transition networks for the comprehensive characterisation of complex conformational change in proteins**. *J Chem Theory Comput* 2006, **2**:840-857.

50. Bussi G, Gervasio FL, Laio A, Parrinello M: **Free-energy landscape for beta hairpin folding from combined parallel tempering and metadynamics**. *J Am Chem Soc* 2006, **128**:13435-13441.

51. Singhal N, Snow CD, Pande VS: **Using path sampling to build better Markovian state models: predicting the folding rate and mechanism of a tryptophan zipper beta hairpin**. *J Chem Phys* 2004, **121**:415-425.

52. Allen RJ, Frenkel D, Wolde PRT: **Simulating rare events in equilibrium or nonequilibrium stochastic systems**. *J Chem Phys* 2006, **124**:024102.

53. Chodera JD, Dill KA, Singhal N, Pande VS, Swope WC, Pitera JW: **Automatic discovery of metastable states for the construction of Markov models of macromolecular conformational dynamics**. *J Chem Phys* 2007, **126**:155101.

54. Kuczera K, Jas GS, Elber R: **Kinetics of helix unfolding: molecular dynamics simulations with milestoning**. *J Phys Chem A* 2009, **113**:7461-7473.

55. Zagrovic B, Sorin EJ, Pande V: **Beta-hairpin folding simulations in atomistic detail using an implicit solvent model**. *J Mol Biol* 2001, **313**:151-159.

56. Wei G, Mousseau N, Derreumaux P: **Complex folding pathways in a simple β-hairpin**. *Proteins Struct Funct Bioinf* 2004, **56**:464-474.

57. Bolhuis PG: **Kinetic pathways of beta-hairpin (un)folding in explicit solvent**. *Biophys J* 2005, **88**:50-61.

58. Du D, Tucker MJ, Gai F: **Understanding the mechanism of beta-hairpin folding via phi-value analysis**. *Biochemistry* 2006, **45**:2668-2678.

59. • Yang S, Onuchic JN, García AE, Levine H: **Folding time predictions from all-atom replica exchange simulations**. *J Mol Biol* 2007, **372**:756-763.
Folding times are predicted for a β-hairpin by combining picosecond molecular dynamics from replica exchange simulations to provide the drift velocity and diffusion coefficient for stochastic dynamics.

60. Cavalli A, Haberthür U, Paci E, Caflisch A: **Fast protein folding on downhill energy landscape**. *Protein Sci* 2003, **12**:1801-1803.

61. • Chung HS, Louis JM, Eaton WA: **Experimental determination of upper bound for transition path times in protein folding from single-molecule photon-by-photon trajectories**. *Proc Natl Acad Sci U S A* 2009, **106**:11837-11844.
New single molecule experiments provide an upper bound to the time taken for actual folding transitions in the 56-residue protein GB1 immobilised on a surface. The data provide a new possibility for comparisons with computer simulation.

62. Itzhaki LS, Otzen DE, Fersht AR: **The structure of the transition state for folding of chymotrypsin inhibitor 2 analyzed by protein engineering methods: evidence for a nucleation-condensation mechanism for protein folding**. *J Mol Biol* 1995, **254**:260-288.

63. Shimada J, Shakhnovich EI: **The ensemble folding kinetics of protein G from an all-atom Monte Carlo simulation**. *Proc Natl Acad Sci U S A* 2002, **99**:11175-11180.

64. Wales DJ: **A microscopic basis for the global appearance of energy landscapes**. *Science* 2001, **293**:2067-2069.